Expanded View Figures

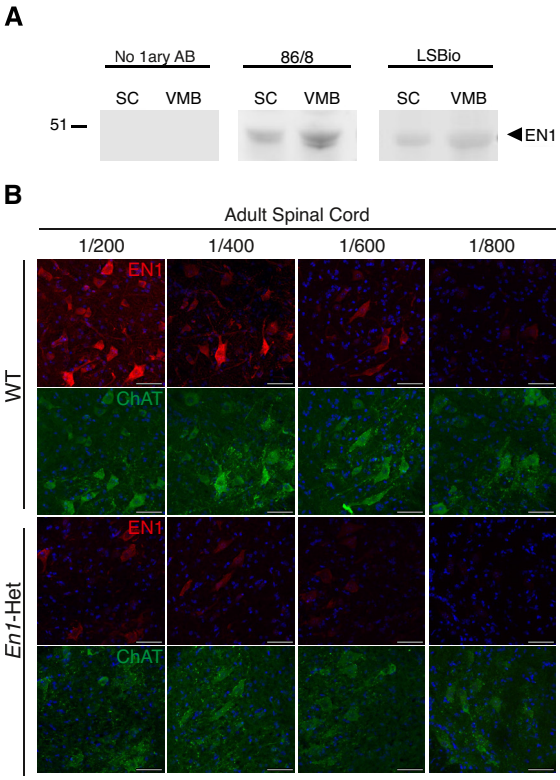

Figure EV1. Characterization of the anti-EN1 LSBio antibody.

A Western blots of spinal cord (SC) and ventral midbrain (VMB) extracts demonstrating that the 86/8 and LSBio antibodies recognize in both structures the same protein migrating with recombinant EN1 velocity. No staining is observed in the absence of primary antibody (left panel). This experiment was performed twice.

B Double staining of 3-month-old WT and *En1*-Het ventral MNs with the anti-ChAT antibody and the anti-EN1 LSBio antibody at various dilutions. EN1 staining decreases with increasing dilutions of the antibody. The loss of staining is more rapid in *En1*-Het than in WT mice. Scale bar = 50 μm.

Data information: This experiment was performed once.

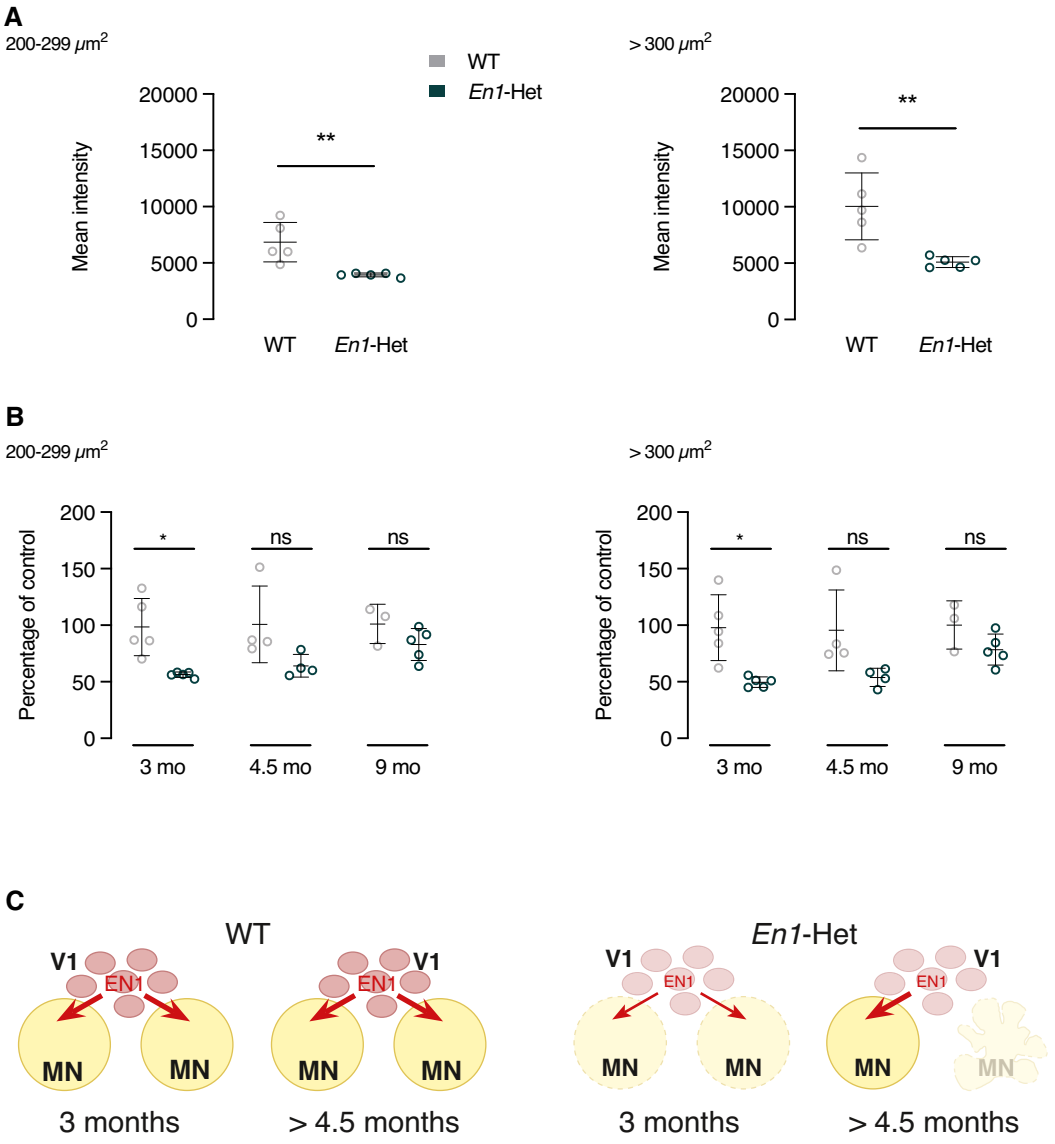

Figure EV2. Evolution of EN1 content per MN in WT and *En1*-Het mice.

A Analysis of EN1 amount in MNs at 3 months in WT and *En1*-Het mice. EN1 content is reduced by about half in γMNs (left panel) and αMNs (right panel). EN1 was revealed by the LSBio antibody allowing for the visualization of endogenous EN1. Unpaired two-sided *t*-test with equal SD (**$P < 0.005$; $n = 5$). Values are mean ± SD.

B Quantification of EN1 amount in γMNs and αMNs with the LSBio antibody at 3, 4.5 and 9 months in WT and *En1*-Het mice. Values at 3 months correspond to the ones shown in panel A. At 4.5 and 9 months, the amount of EN1 in MNs is similar in *En1*-Het and WT mice suggesting that, with time, each remaining MN receives a higher amount of EN1. Two-way ANOVA showed a significant main effect for the γMNs ($F(1, 20) = 16.93$, $P = 0.0005$) and αMNs ($F(1, 20) = 19.03$, $P = 0.0003$). Unpaired two-sided *t*-test with equal SD (*$P < 0.05$; $n = 4$–5). Data information: This experiment was performed once. Values are mean ± SD.

C Hypothetical representation of EN1 availability to αMNs in WT and Het mice. In the *En1*-Het mouse, each V1 interneurons only provides half as much EN1 to the full population of αMNs at 3 months of age. At 4.5 months of age and later, half of the αMNs have been lost allowing each remaining αMN to receive its full complement of EN1 from the V1 interneurons.

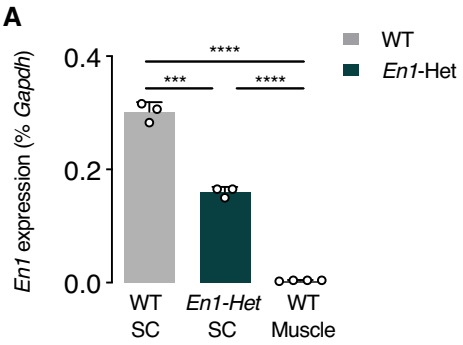

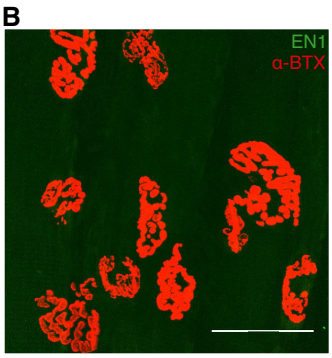

Figure EV3. Absence of *En1* transcription or EN1 protein at endplate level.

A RT–qPCR of RNA from the lumbar enlargement at 4.5 months of WT and *En1*-Het mice and from WT muscle. *En1* expression is absent from the muscle of WT mice. Unpaired two-sided *t*-test with equal SD (***$P < 0.005$; ****$P < 0.0005$; $n = 4$–5). Values are mean ± SD.

B Immunohistochemistry for EN1 protein (LSBio antibody, in green) shows its absence at the level of the NMJ (α-BTX, in red). Scale bar = 50 μm.

Data information: This experiment was done once. Values are mean ± SD.

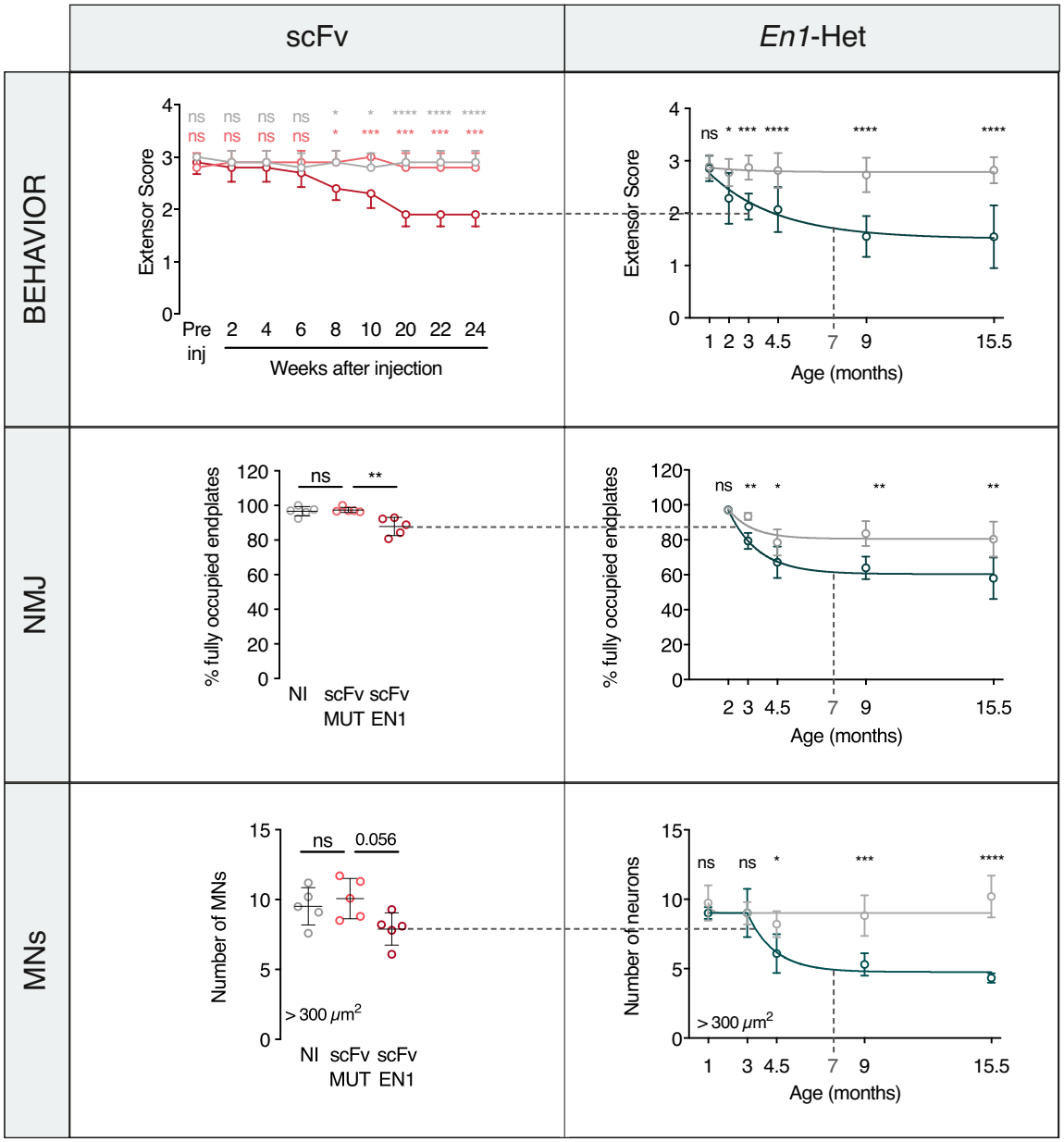

Figure EV4. Comparison of *En1*-Het and scFvEN1-expressing mice phenotypes.

Comparison between En1-het mouse and scFvEN1 models. Data and graphs are from main figures (primarily Figs 2 and 4). WT mice injected with scFvEN1 show similar results to those obtained in the *En1*-Het mouse with a milder strength loss, a smaller decrease in the number of fully occupied endplates, and the specific loss of large-size αMNs. At 7 months, scFvEN1 injected mice have a phenotype similar to 3-month-old *En1*-Het mice.